Cooperative Adaptive Cruise Control: Network-Aware Analysis of String Stability

Sinan Öncü, Jeroen Ploeg, Nathan van de Wouw, and Henk Nijmeijer, *Fellow, IEEE*

***Abstract*—In this paper, we consider a Cooperative Adaptive Cruise Control (CACC) system, which regulates intervehicle distances in a vehicle string, for achieving improved traffic flow stability and throughput. Improved performance can be achieved by utilizing information exchange between vehicles through wireless communication in addition to local sensor measurements. However, wireless communication introduces network-induced imperfections, such as transmission delays, due to the limited bandwidth of the network and the fact that multiple nodes are sharing the same medium. Therefore, we approach the design of a CACC system from a Networked Control System (NCS) perspective and present an NCS modeling framework that incorporates the effect of sampling, hold, and network delays that occur due to wireless communication and sampled-data implementation of the CACC controller over this wireless link. Based on this network-aware modeling approach, we develop a technique to study the so-called *string stability* property of the string, in which vehicles are interconnected by a vehicle following control law and a constant time headway spacing policy. This analysis technique can be used to investigate tradeoffs between CACC performance (string stability) and network specifications (such as delays), which are essential in the multidisciplinary design of CACC controllers. Finally, we demonstrate the validity of the presented framework in practice by experiments performed with CACC-equipped prototype vehicles.**

***Index Terms*—Cooperative Adaptive Cruise Control (CACC), networked control systems (NCS), string stability.**

I. Introduction

THE ever-increasing demand for mobility in today's life brings additional burden on the existing ground transportation infrastructure, for which a feasible solution in the near future lies in more efficient use of currently available means of transportation. For this purpose, development of Intelligent Transportation Systems (ITS) technologies that contribute to improved traffic flow stability, throughput, and safety is needed. Cooperative Adaptive Cruise Control (CACC), being one of the promising ITS technologies, extends the currently available Adaptive Cruise Control (ACC) technology with the addition of information exchange between vehicles through Vehicle-to-Vehicle (V2V) and Vehicle-to-Infrastructure (V2I) wireless communication [1].

In today's traffic, limited human perception of traffic conditions and human reaction characteristics constrain the lower limits of achievable safe intervehicle distances. In addition, erroneous human driving characteristics may cause traffic flow instabilities, which result in so-called shockwaves. In dense traffic conditions, a single driver overreacting to a momentary disturbance (e.g., a slight deceleration of the predecessor) can trigger a chain of reactions in the rest of the follower vehicles. The amplification of such a disturbance can bring the traffic to a full stop kilometers away from the disturbance source and cause traffic jams for no apparent reason. For this reason, the attenuation of disturbances across the vehicle string, which is covered by the notion of *string stability*, is an essential requirement for vehicle platooning. Wireless information exchange between vehicles provides the means for overcoming sensory limitations of human- or ACC-operated vehicles and, therefore, can contribute significantly to improving the traffic flow, particularly on highways.

One of the earliest studies toward regulating intervehicle distances to achieve improved traffic flow dates back to the 1960s, in which the authors formulated the problem in an optimal control design framework [2]. In following years, many practical issues regarding a successful implementation were addressed particularly in the scope of the California Partners for Advanced Transportation tecHnology (PATH) program, such as different intervehicle spacing strategies and information flow structures [3], heterogeneous traffic conditions [4], communication delays [5], and actuator limitations [6]. In [7] and [8], the problem was approached from a large-scale system perspective, and the inclusion principle was used to decompose the interconnected vehicle string into subsystems with overlapping states, for which decentralized controllers were designed. Some research has focused on making use of underlying interconnection structures to derive scalable system theoretic properties for this type of platoon systems [9], [10]. More recently, proof-of-concept demonstrations with CACC vehicles have been performed with homogeneous vehicle strings [11] and also with heterogeneous vehicle strings in a multivendor setting [12], [13]. Significant improvements over existing ACC technology can be achieved

Manuscript received April 18, 2013; revised November 20, 2013; accepted January 9, 2014. Date of publication February 24, 2014; date of current version August 1, 2014. This work was supported in part by the High Tech Automotive Systems Program through the Connect and Drive Project and in part by the European 7th Framework Network of Excellence: Highly complex and networked control systems (HYCON2) under Grant 257462. The Associate Editor for this paper was L. Vlacic.

S. Öncü was with the Department of Mechanical Engineering, Eindhoven University of Technology, 5600 MB Eindhoven, The Netherlands. He is now with the Integrated Vehicle Safety Department, Netherlands Organization for Applied Scientific Research (TNO) Technical Sciences, 5700 AT Helmond, The Netherlands (e-mail: sinan.oncu@tno.nl).

J. Ploeg is with the Integrated Vehicle Safety Department, Netherlands Organisation for Applied Scientific Research (TNO) Technical Sciences, 5700 AT Helmond, The Netherlands, and also with the Department of Mechanical Engineering, Eindhoven University of Technology, 5600 MB Eindhoven, The Netherlands (e-mail: jeroen.ploeg@tno.nl).

N. van de Wouw and H. Nijmeijer are with the Department of Mechanical Engineering, Eindhoven University of Technology, 5600 MB Eindhoven, The Netherlands (e-mail: n.v.d.wouw@tue.nl; h.nijmeijer@tue.nl).

Color versions of one or more of the figures in this paper are available online at http://ieeexplore.ieee.org.

Digital Object Identifier 10.1109/TITS.2014.2302816

already with relatively simple control algorithms and communication structures, but implementation for real traffic conditions requires consideration of the constraints imposed by the wireless communication needed to implement CACC.

In this paper, we approach the problem of regulating intervehicle distances in a CACC system from a Networked Control System (NCS) perspective. In the fields of NCS, one considers the control of systems over a communication network [14], [15]. Control over a wireless communication network is the enabling technology that makes CACC realizable; however, very few studies consider the imperfections that are introduced by the network [5], [16], [22], [23]. This is mainly due to the fact that systematic NCS tools have arisen relatively recently. In [5], a continuous-time transfer-function-based analysis of the effects of constant time delays on string stability was carried out. Here, we adopt a discretization-based NCS modeling and analysis approach, which also incorporates the effects of the sampling and the zero-order hold (ZOH) in addition to constant wireless communication delays. We extend the results in [22] with real experiments. The interconnected vehicle string model presented in this paper has also been used in [23] for providing conditions on the uncertain and time-varying sampling/transmission intervals and delays, under which string stability can still be guaranteed.

The main purpose of this paper is to emphasize the necessity for considering CACC in a NCS framework by studying the effects of wireless communication on the performance of an existing CACC controller in terms of string stability. Moreover, we also show how these string stability analyses can provide the designer with guidelines for making the tradeoffs between control and network specifications. The reliability of the presented framework is demonstrated with experiments, which were carried out on a test track with CACC-instrumented prototype vehicles.

In Section II, we introduce the general control objective and the string stability requirement. In Section III, the underlying longitudinal vehicle dynamics and the control structure are presented, which together form the CACC vehicle model that will be used in the rest of the paper. Subsequently, we use this CACC vehicle model to construct the interconnected vehicle string model. In the latter model, we consider the local (ACC) sensor measurements as internal dynamics of the interconnected system and focus on the effects of network imperfections on the wirelessly communicated data. In Section IV, we present the CACC NCS model and construct a discrete-time interconnected system model that incorporates the vehicle dynamics, the CACC controller, and the network-induced effects. In Section V, we present the frequency-response-based string stability analysis and obtain maximum allowable time delays for different controller and network parameters. In Section VI, we demonstrate the practical validity of these results with experiments by using CACC-equipped prototype vehicles. Section VII closes the paper with conclusions.

II. Problem Formulation

The general objective of a CACC system is to pack the driving vehicles together as tightly as possible, in order to increase traffic throughput while preventing amplification of disturbances throughout the string; the latter of which is known as string instability [3], [17]. These are two conflicting objectives when conventional methods are considered, since reducing intervehicle distance results in shockwaves (due to string instability), which adversely affect the global traffic flow. Other important requirements are related to safety, comfort, and fuel consumption, but these are not considered in the scope of this paper.

A. Vehicle Following Objective

The vehicles forming the platoon are interconnected through the vehicle following objective. Each vehicle is requested to follow its predecessor while maintaining a desired, but not necessarily constant, distance. Here, we consider a constant time headway spacing policy, where the desired spacing $(d_{r,i})$ between the front bumper of the ith vehicle to its predecessor's rear bumper is given by

$$d_{r,i} = r_i + h_{d,i} v_i \tag{1}$$

where i is the vehicle index; r_i is a constant term that forms the gap between consecutive vehicles at standstill; $h_{d,i}$ is the headway-time constant, representing the time that it will take the ith vehicle to arrive at the same position as its predecessor when $r_i = 0$; and v_i is the vehicle velocity. The actual distance between two consecutive vehicles (d_i) is given by

$$d_i = q_{i-1} - (q_i + L_i) = q_{i-1} - q_i \tag{2}$$

where q_i is the absolute position of the ith vehicle in global coordinates in the longitudinal direction (i.e., 1-D translational coordinates), and L_i is the vehicle length. The local control objective, which is referred to as vehicle following, can now be defined as regulating the error

$$e_i = d_i - d_{r,i} \tag{3}$$

to zero.

B. String Stability

An additional requirement, i.e., so-called string stability, involves the global performance of the CACC vehicle string, with regard to attenuation of disturbances along the vehicle string, and is evaluated by considering amplification of signals such as the distance error, the velocity, the acceleration, or the control effort in the vehicle string as the vehicle index increases.

Hence, stability is not only studied in the time domain but also in the spatial domain. This property is commonly called *string stability*, [3], [5], [17], [18], and can be quantified by the magnitude of the string stability transfer function

$$SS_{\Delta_i}(s) = \frac{\Delta_i(s)}{\Delta_{i-1}(s)}, \qquad i \geq 1,\ s \in \mathbb{C} \tag{4}$$

where $\Delta_i(s) := \mathcal{L}(\delta_i),\ \delta_i \in \mathbb{R}$ is the signal of interest for the evaluation of string stability, and $\mathcal{L}$ denotes the Laplace operator. The string stability requirement can be interpreted as a condition on the maximal amplification of perturbations along

the string. This maximum amplification can be represented by the H-infinity norm of the string stability transfer function

$$\|SS_{\Delta_i}(jw)\|_\infty = \sup_{\omega\in\mathbb{R}} \|SS_{\Delta_i}(jw)\|. \tag{5}$$

In accordance with [5] and [18], we formulate the following condition for string stability:

$$\|SS_{\Delta_i}(jw)\|_\infty \leq 1 \ \forall\omega, \quad i \geq 1. \tag{6}$$

III. Interconnected Vehicle String Model

Here, the underlying longitudinal vehicle dynamics and the control structure are presented, which together form the CACC vehicle model. Subsequently, we use this CACC vehicle model to construct the interconnected vehicle string model.

A. Longitudinal Vehicle Dynamics Model With Actuator Delay

We use the following linearized third-order state-space representation of the longitudinal dynamics for each vehicle in the string:

$$\begin{aligned} \dot{q}_i(t) &= v_i(t) \\ \dot{v}_i(t) &= a_i(t) \\ \dot{a}_i(t) &= -\eta_i^{-1} a_i(t) + \eta_i^{-1}\tilde{u}_i(t) \end{aligned} \tag{7}$$

where $q_i(t)$, $v_i(t)$, $a_i(t)$ are the absolute position, velocity, and acceleration, respectively; η_i represents a parameter characterizing the internal actuator dynamics; and $\tilde{u}_i$ is the commanded acceleration for the ith vehicle. This model is widely used in the literature as a basis for analysis [5], [11], [18]. Here, we extend this model with an additional constant actuation delay $(\tau_{a,i})$ between the desired acceleration (u_i) and the commanded acceleration

$$\tilde{u}_i(t) = u_i(t - \tau_{a,i}) \tag{8}$$

to account for delays in the throttle actuation. Equivalently, by using Laplace transforms $\mathcal{L}(q_i(t)) =: Q_i(s)$ and $\mathcal{L}(\tilde{u}_i(t)) =: U_i(s)e^{-\tau_{a,i}s}$, the vehicle model can be represented by the transfer function

$$G_i(s) = \frac{Q_i(s)}{U_i(s)} = \frac{1}{s^2(\eta_i s + 1)} e^{-\tau_{a,i}s}, \qquad s \in \mathbb{C}. \tag{9}$$

Note that the notational use of small letters for time-domain signals and capital letters for their frequency-domain counterparts will be retained throughout the rest of the paper.

B. CACC Control Structure

Since the main focus of this paper is to investigate the network effects on the string stability properties of a platooning system, the details of the controller design are omitted in this paper. For more details on the controller, we refer to [18], while information on the experimental validation of this controller with CACC-equipped vehicles can be found in [11].

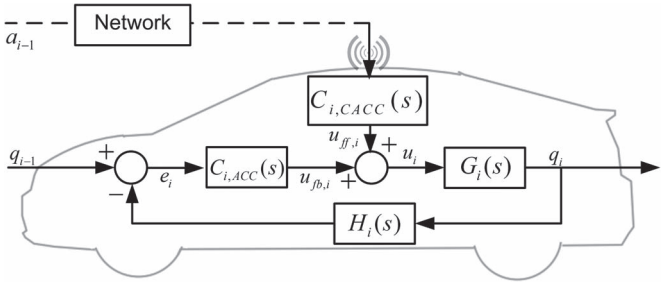

Fig. 1. Control structure block diagram of a single CACC-equipped vehicle.

The control structure for a single CACC-equipped vehicle (vehicle i) is as shown in Fig. 1. CACC operation is introduced as an addition to the underlying ACC in a feedforward fashion. The signal conditioning block $H_i(s) = 1 + h_{d,i}s$ is used to implement the spacing strategy given in (1). The feedback controller $(C_{i,\mathrm{ACC}}(s))$, which constitutes the ACC part, is a proportional and derivative (PD)-type controller that acts on locally sensed data (e.g., using radar) to achieve the vehicle following objective, and it is given in the Laplace domain as follows:

$$U_{\mathrm{fb},i}(s) = C_{i,\mathrm{ACC}}(s)E_i(s) = \omega_{c,i}(\omega_{c,i} + s)E_i(s) \tag{10}$$

where $\omega_{c,i}$ is the bandwidth of the controller and is chosen such that $\omega_{c,i} \ll w_{g,i} := 1/\eta_i$ holds, in order to prevent actuator saturation. The time-domain equivalent of (10) is obtained by using (3) with (1) and (2) as follows:

$$\begin{aligned} u_{\mathrm{fb},i} &= \omega_{c,i}^2 e_i + \omega_{c,i}\dot{e}_i \\ &= \omega_{c,i}^2 e_i + \omega_{c,i}(v_{i-1} - v_i - h_{d,i}a_i) \end{aligned} \tag{11}$$

where $\omega_{c,i}^2$ and $\omega_{c,i}$ represent the proportional and derivative gains of the ACC controller, respectively. This controller uses the relative distance $(q_i - q_{i-1})$ and relative velocity $(v_i - v_{i-1})$ between the host and the directly preceding vehicle, which are available as sensed measurements through a radar unit that is mounted at the front of the vehicle and local measurements of velocity (v_i) and acceleration (a_i) of the host vehicle.

Additional feedforward action is utilized to improve vehicle following and string stability performance, which forms the CACC part of the controller ($C_{i,\mathrm{CACC}}(s)$ in Fig. 1). It uses the acceleration of the directly preceding vehicle (a_{i-1}). Following the design guidelines in [18], the feedforward filter is given as follows:

$$U_{\mathrm{ff},i}(s) = C_{i,\mathrm{CACC}}(s)A_{i-1}(s) = \frac{1}{H_i(s)G_i(s)s^2}A_{i-1}(s) \tag{12}$$

and achieves zero steady-state vehicle following error (e_i). Now, using $A_{i-1}(s) = s^2Q_{i-1}(s) = s^2G_{i-1}(s)U_{i-1}(s)$, (12) can be rewritten as follows:

$$U_{\mathrm{ff},i}(s) = \frac{1}{H_i(s)G_i(s)}G_{i-1}(s)U_{i-1}(s). \tag{13}$$

For a homogeneous vehicle string (i.e., identical vehicles, and thus $G_i(s) = G_{i-1}(s)\ \forall i$) this reduces to

$$U_{\mathrm{ff},i}(s) = \frac{1}{H_i(s)}U_{i-1}(s) = \frac{1}{1 + h_{d,i}s}U_{i-1}(s). \tag{14}$$

Here, it can be seen that additional dynamics is introduced in the controller due to the velocity-dependent spacing policy in (1), which gives the following time-domain representation for the CACC feedforward filter in (14):

$$\dot{u}_{\mathrm{ff},i} = -h_{d,i}^{-1} u_{\mathrm{ff},i} + h_{d,i}^{-1} u_{i-1}. \tag{15}$$

The time-domain representations of the CACC controller in (11) and (15) will be used in the state-space representation of the CACC vehicle model presented next.

C. Closed-Loop CACC Model

The general form of the closed-loop CACC vehicle model is obtained by combining the vehicle longitudinal dynamics in (7) with the distance error equation in (3), the feedback control law (11), and the feedforward control law (15). In doing so, we replace u_{i-1} by $\hat{u}_{i-1}$, where $\hat{u}_{i-1}$ denotes the fact that u_{i-1} is transmitted over the network. Note that $\hat{u}_{i-1}$ typically differs from u_{i-1} due to network-introduced effects (such as sampling, hold, and delays).

By choosing the state variables as $x_i^T = [e_i \ v_i \ a_i \ u_{\mathrm{ff},i}] \in \mathbb{R}^{n_x}$, the ith CACC-equipped vehicle dynamics $(2 \leq i \leq n)$ in an n-vehicle string is described by

$$\dot{x}_i = A_{i,i} x_i + A_{i,i-1} x_{i-1} + B_{s,i} \tilde{u}_i + \underbrace{B_{c,i} \hat{u}_{i-1}}_{wireless}$$

$$A_{i,i} = \begin{bmatrix} 0 & -1 & -h_{d,i} & 0 \\ 0 & 0 & 1 & 0 \\ 0 & 0 & -\eta_i^{-1} & 0 \\ 0 & 0 & 0 & -h_{d,i}^{-1} \end{bmatrix} \quad B_{s,i} = \begin{bmatrix} 0 \\ 0 \\ \eta_i^{-1} \\ 0 \end{bmatrix}$$

$$A_{i,i-1} = \begin{bmatrix} 0 & 1 & 0 & 0 \\ 0 & 0 & 0 & 0 \\ 0 & 0 & 0 & 0 \\ 0 & 0 & 0 & 0 \end{bmatrix} \quad B_{c,i} = \begin{bmatrix} 0 \\ 0 \\ 0 \\ h_{d,i}^{-1} \end{bmatrix} \tag{16}$$

where $B_{s,i}$ is the input vector corresponding to the input $\tilde{u}_i$, which is generated by using locally available (sensed) data, and $B_{c,i}$ is the input vector for the additional CACC input $\hat{u}_{i-1}$, which is sent to the ith vehicle through the wireless network and is therefore subject to network effects.

The next step in formulating the model is the inclusion of the actuator behavior expressed by the delay $\tau_{a,i}$ in the relation between u_i and $\tilde{u}_i$ [see (8)]. Note that the transfer function $e^{-\tau_{a,i} s}$ in (9) of the actuator delay in (8) is nonrational and renders the model infinite-dimensional. In Section IV, we will pursue a discrete-time modeling approach for the modeling of the *networked* CACC-controlled vehicle string relying on finite-dimensional models of the vehicle dynamics. To support this approach, we approximate the delay transfer function $e^{-\tau_{a,i} s}$ by a rational transfer function based on Padé approximations [19]. This leads to the following state-space representation of the κth-order Padé approximation of the actuator delay:

$$\begin{aligned} \dot{\tilde{p}}_i &= A_{p,i} \tilde{p}_i + B_{p,i} u_i \\ \tilde{u}_i &= C_{p,i} \tilde{p}_i + D_{p,i} u_i \end{aligned} \tag{17}$$

with $\tilde{p}_i = [p_{i,1} \ p_{i,2} \ \ldots \ p_{i,\kappa}]^T \in \mathbb{R}^{\kappa}$.

The longitudinal vehicle dynamics with actuator delay is obtained by using the augmented state vector $\tilde{x}_i^T = [x_i^T \ \tilde{p}_i^T]$ in (16) together with (17) to obtain the total vehicle dynamics model

$$\dot{\tilde{x}}_i = \tilde{A}_{i,i} \tilde{x}_i + \tilde{A}_{i,i-1} \tilde{x}_{i-1} + \tilde{B}_{s,i} u_i + \tilde{B}_{c,i} \hat{u}_{i-1}, \ 2 \leq i \leq n$$

$$\tilde{A}_{i,i} = \begin{bmatrix} A_{i,i} & B_{s,i} C_{p,i} \\ 0 & A_{p,i} \end{bmatrix} \quad \tilde{B}_{s,i} = \begin{bmatrix} B_{s,i} D_{p,i} \\ B_{p,i} \end{bmatrix}$$

$$\tilde{A}_{i,i-1} = \begin{bmatrix} A_{i,i-1} & 0 \\ 0 & 0 \end{bmatrix} \quad \tilde{B}_{c,i} = \begin{bmatrix} B_{c,i} \\ 0 \end{bmatrix}. \tag{18}$$

A time-domain representation of the CACC feed-back/forward control input with the given spacing policy is given as follows:

$$\begin{aligned} u_i &= u_{\mathrm{fb},i} + u_{\mathrm{ff},i}, \qquad 1 \leq i \leq n \\ &= K_{i,i-1} x_{i-1} + K_{i,i} x_i \end{aligned}$$

$$K_{i,i-1} = \begin{bmatrix} 0 \\ \omega_{c,i} \\ 0 \\ 0 \end{bmatrix}^T \quad K_{i,i} = \begin{bmatrix} \omega_{c,i}^2 \\ -\omega_{c,i} \\ -\omega_{c,i} h_{d,i} \\ \nu \end{bmatrix}^T \tag{19}$$

where $\nu = 1$ corresponds to an operational CACC, and $\nu = 0$ gives only ACC. For more details on the CACC setup, see [11] and [18].

D. Interconnected Vehicle String Model

Here, the closed-loop CACC model for the individual vehicle, as proposed in the previous section, is employed to construct the interconnected vehicle string model. In order to do so, a reference vehicle (denoted by index $i = 0$ and with state x_0) is introduced, which may represent either the rest of the traffic as seen by the lead vehicle (with index $i = 1$) in the string or the trajectory generator in the lead vehicle in case there are no preceding vehicles. The dynamics of the lead vehicle, without actuator delay, is described by

$$\dot{x}_0 = A_0 x_0 + B_{s,0} u_r$$

$$A_0 = \begin{bmatrix} 0 & 0 & 0 & 0 \\ 0 & 0 & 1 & 0 \\ 0 & 0 & -\eta_0^{-1} & 0 \\ 0 & 0 & 0 & 0 \end{bmatrix} \quad B_{s,0} = \begin{bmatrix} 0 \\ 0 \\ \eta_0^{-1} \\ 0 \end{bmatrix} \tag{20}$$

where $x_0 = [e_0, v_0, a_0, u_{\mathrm{ff},0}]^T$, and u_r is the reference acceleration profile. In (20), the state variables are chosen in accordance with those for the real vehicles in the string in (16). Consequently, redundant states exist in (20), but nevertheless, we opt for this representation as it results in a uniform representation for the upcoming vehicle string model. In addition, the lead vehicle (with state x_1) in the string requires special consideration. The CACC input is locally available to this vehicle without any network-induced imperfection since it is generated locally by this vehicle. By considering these two special cases for the reference $(i = 0)$ and the lead $(i = 1)$ vehicles and using the CACC vehicle model in (18) for each operational CACC

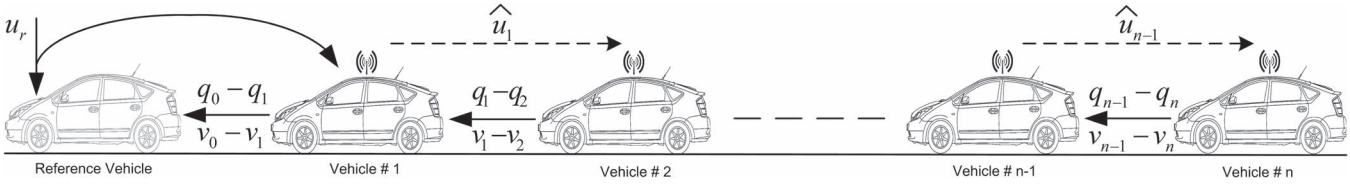

Fig. 2. Schematic representation of the n-vehicle string.

subsystem $(i \geq 2)$, we obtain the following equations for an n-vehicle string, as shown in Fig. 2:

$$\begin{aligned}
\dot{\tilde{x}}_0 &= \tilde{A}_0\tilde{x}_0 + B_{s,0}u_r \\
\dot{\tilde{x}}_1 &= \tilde{A}_{1,1}\tilde{x}_1 + \tilde{A}_{1,0}\tilde{x}_0 + \tilde{B}_{s,1}u_1 + \tilde{B}_{c,1}u_r \\
\dot{\tilde{x}}_2 &= \tilde{A}_{2,2}\tilde{x}_2 + \tilde{A}_{2,1}\tilde{x}_1 + \tilde{B}_{s,2}u_2 + \tilde{B}_{c,2}\hat{u}_1 \\
&\vdots \\
\dot{\tilde{x}}_n &= \tilde{A}_{n,n}\tilde{x}_n + \tilde{A}_{n,n-1}\tilde{x}_{n-1} + \tilde{B}_{s,n}u_n + \tilde{B}_{c,n}\hat{u}_{n-1} \qquad (21)
\end{aligned}$$

where extended state vectors $\tilde{x}_0$ and $\tilde{x}_1$ are used here, indicating the inclusion of Padé approximations for the actuator delay in both vehicles 0 and 1.

By defining a new state vector $\bar{x}_n = [\tilde{x}_0^T\ \tilde{x}_1^T\ \tilde{x}_2^T\ \cdots\ \tilde{x}_n^T]^T$, we lump n subsystems together with the reference model $(\tilde{x}_0)$ and use the input of the reference vehicle model (u_r) as the exogenous input to the cascaded system, which can now be represented as

$$\dot{\bar{x}}_n = \bar{A}_n\bar{x}_n + \bar{B}_{s,n}\bar{u}_n + \bar{B}_{c,n}\hat{\bar{u}}_n + B_r u_r \qquad (22)$$

with

$$\bar{A}_n = \begin{bmatrix} \tilde{A}_0 & 0 & 0 & \cdots & 0 \\ \tilde{A}_{1,0} & \tilde{A}_{1,1} & 0 & \cdots & 0 \\ 0 & \tilde{A}_{2,1} & \tilde{A}_{2,2} & \cdots & 0 \\ \vdots & & \ddots & \ddots & \vdots \\ 0 & \cdots & 0 & \tilde{A}_{n,n-1} & \tilde{A}_{n,n} \end{bmatrix}$$

$$\bar{B}_{s,n} = \begin{bmatrix} 0 & \cdots & \cdots & 0 \\ \tilde{B}_{s,1} & 0 & \cdots & 0 \\ 0 & \tilde{B}_{s,2} & & \vdots \\ \vdots & & \ddots & 0 \\ 0 & \cdots & 0 & \tilde{B}_{s,n} \end{bmatrix} \quad B_r = \begin{bmatrix} \tilde{B}_{s,0} \\ \tilde{B}_{c,1} \\ 0 \\ \vdots \\ 0 \end{bmatrix}$$

$$\bar{B}_{c,n} = \begin{bmatrix} 0 & \cdots & 0 & 0 \\ 0 & \cdots & 0 & 0 \\ \tilde{B}_{c,2} & \cdots & 0 & 0 \\ \vdots & \ddots & \vdots & \vdots \\ 0 & \cdots & \tilde{B}_{c,n} & 0 \end{bmatrix}$$

and $\hat{\bar{u}}_n = [\hat{u}_1\ \hat{u}_2\ \ldots\ \hat{u}_n]^T$ with $\bar{u}_n = [u_1\ u_2\ \ldots\ u_n]^T$. The control law in (19), i.e., $u_i = [K_{i,i-1}\ K_{i,i}][x_{i-1}^T\ x_i^T]^T$, for each subsystem $i \in \{1, 2, \ldots, n\}$, can now be incorporated in (22) by using

$$\bar{u}_n = \bar{K}_n\bar{x}_n \qquad (23)$$

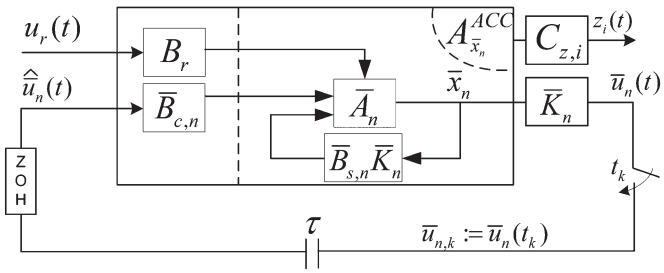

Fig. 3. NCS model.

with

$$\bar{K}_n = \begin{bmatrix} K_{1,0} & K_{1,1} & 0 & \cdots & 0 \\ 0 & K_{2,1} & K_{2,2} & \cdots & 0 \\ \vdots & & \ddots & \ddots & \vdots \\ 0 & \cdots & & K_{n,n-1} & K_{n,n} \end{bmatrix}. \qquad (24)$$

In the resulting interconnected vehicle string model (22), (23), the wirelessly communicated control commands $\hat{\bar{u}}_n$ are kept separate for future analysis.

Let us now formulate the closed-loop CACC vehicle string model in (22) and (23), in a more compact form. Previously, the interconnected vehicle string was formulated such that the control inputs (i.e., $\bar{u}_n$ for ACC and additionally $\hat{\bar{u}}_n$ for CACC) are kept separate, according to their way of being acquired by the host vehicle (i.e., through direct measurement or through wireless communication). In addition, the model permits to express the CACC control commands, which are actually feedforward signals from one vehicle to the next, as state-feedback control laws. Now, we adopt the realistic assumption that a much higher sampling rate is employed for the locally sensed data used for the ACC functionality than for the wirelessly communicated CACC commands and, hence, model the ACC vehicle following controller as an inherently continuous-time dynamic coupling between vehicles. This results in the following reformulation, which allows us to analyze in detail the effects of wireless communication inputs:

$$\begin{aligned}
\dot{\bar{x}}_n &= (\bar{A}_n + \bar{B}_{s,n}\bar{K}_n)\bar{x}_n + \bar{B}_{c,n}\hat{\bar{u}}_n + B_r u_r \\
&= A_{\bar{x}_n}^{\mathrm{ACC}}\bar{x}_n + \bar{B}_{c,n}\hat{\bar{u}}_n + B_r u_r. \qquad (25)
\end{aligned}$$

Note that, if $\hat{\bar{u}}$ is omitted in (25), then one obtains the ACC closed-loop vehicle string model.

IV. Networked CACC Model

Here, we will complete the model with network aspects, such as sampling, hold, and delays, induced by wireless communication and therewith derive a networked CACC vehicle string model. The related CACC NCS model schematic is shown in Fig. 3. The signal $\bar{u}_n$ is sent over the wireless network after

being sampled at sampling instants $t_k = kh$, where h is the constant sampling interval. Note that these sampled data are sent over the wireless network to be used for the implementation of CACC and, hence, are typically subject to network-induced delays. These wireless communication delays are mainly affected by the number of vehicles that share the same network (i.e., reside in the same platoon). Given the fact that the number of vehicles in a platoon varies on a slow timescale and, hence, has typically much slower dynamics than the one of the vehicle string, delays can be considered as constant for string stability analysis. Here, we consider constant, although uncertain and possibly large, network-induced delays τ that are modeled as

$$\tau = \tau^* + (l-1)h, \qquad l \in \{1,2,3,\ldots\}, \quad \tau^* \in [0,h]. \tag{26}$$

By large delays, we indicate delays that are larger than the sampling interval h (obtained in (26) for $l > 1$). The ZOH device (see Fig. 3), transforming the delayed discrete-time control command $\bar{u}_{n,k}$ to the continuous-time control command $\hat{\bar{u}}(t)$ implemented at the vehicle, responds instantaneously to newly arrived data. Using the CACC model given in the previous section, the continuous-time CACC NCS model for an n-vehicle string becomes

$$\begin{aligned} \dot{\bar{x}}_n &= A^{\mathrm{ACC}}_{\bar{x}_n}\bar{x}_n + \bar{B}_{c,n}\hat{\bar{u}}_n + B_r u_r \\ \hat{\bar{u}}_n(t) &= \bar{u}_{n,k-l+1}, \qquad t \in [t_k+\tau^*, t_{k+1}+\tau^*] \end{aligned} \tag{27}$$

where $\bar{u}_{n,k} := \bar{u}_n(t_k)$ and $A^{\mathrm{ACC}}_{\bar{x}_n} = \bar{A}_n + \bar{B}_{s,n}\bar{K}_n$. We care to stress here that this model takes the effects of sampling, hold, and delays due to communication over the wireless network explicitly into account. Next, we will derive a discrete-time CACC NCS model to be used for string stability analysis in Section V. Inspired by the work in [20] and [21], the following discrete-time CACC NCS model description is based on exact[1] discretization of (27) at the sampling instants $t_k = kh$ by using $\bar{x}_{n,k} := \bar{x}_n(t_k)$, $k \in \mathbb{N}$:

$$\begin{aligned} \bar{x}_{n,k+1} = e^{A^{\mathrm{ACC}}_{\bar{x}_n}h}\bar{x}_{n,k} + \int_0^{h-\tau^*} e^{A^{\mathrm{ACC}}_{\bar{x}_n}s} ds \bar{B}_{c,n}\bar{u}_{n,k-l+1} \\ + \int_{h-\tau^*}^{h} e^{A^{\mathrm{ACC}}_{\bar{x}_n}s} ds \bar{B}_{c,n}\bar{u}_{n,k-l} + \int_0^h e^{A^{\mathrm{ACC}}_{\bar{x}_n}s} ds B_r u_{r,k}. \end{aligned} \tag{28}$$

Next, we formulate this discrete-time model in state-space form using the augmented state vector $\xi_k = [\bar{x}^T_{n,k}\ \bar{u}^T_{n,k-1}\ \bar{u}^T_{n,k-2}\ \cdots\ \bar{u}^T_{n,k-l}]^T$, as also employed in [20]. Then, the discrete-time CACC NCS model is given by

$$\xi_{k+1} = A_\xi(\tau,h)\xi_k + B_\xi(\tau,h)\bar{u}_{n,k} + \Gamma_r(h)u_{r,k} \tag{29}$$

[1]This discretization is exact for a piecewise constant sampled approximation of the input signal u_r at the sampling frequency $1/h$, which is considered sufficiently accurate given the fact that this signal is typically low-frequent in practice; see also Section VI.

with

$$\begin{aligned} A_\xi(\tau,h) &= \begin{bmatrix} e^{A^{\mathrm{ACC}}_{\bar{x}_n}h} & M_{l-1} & M_{l-2} & \cdots & M_0 \\ 0 & 0 & 0 & \cdots & 0 \\ 0 & I & 0 & \cdots & 0 \\ \vdots & & \ddots & \cdots & \\ 0 & \cdots & 0 & I & 0 \end{bmatrix} \\ B_\xi(\tau,h) &= [\,M_l^T \quad I \quad 0 \quad \cdots \quad 0\,]^T \\ \Gamma_r(h) &= \int_0^h e^{A^{\mathrm{ACC}}_{\bar{x}_n}s} ds B_r \\ M_j(\tau,h) &= \begin{cases} \int_{h-t_{j+1}}^{h-t_j} e^{A^{\mathrm{ACC}}_{\bar{x}_n}s} ds \bar{B}_{c,n}, & \text{if } 0 \le j \le 1 \\ 0, & \text{if } 1 < j \le l \end{cases} \end{aligned}$$

where $t_0 := 0$, $t_1 = \tau^*$, and $t_2 := h$. The CACC control inputs $\bar{u}_{n,k} = [u_{1,k}\ \ldots\ u_{n,k}]^T$ are sent through the wireless network and will be represented as a full state-feedback control law for the discrete-time model (29) by using the augmented state vector ξ_k as follows:

$$\bar{u}_{n,k} = [\,\bar{K}_n \quad 0_{n\times ln}\,]\,\xi_k = K_\xi \xi_k. \tag{30}$$

Next, we substitute (30) into (29) to obtain the closed-loop CACC NCS model

$$\xi_{k+1} = \overline{A_\xi}(\tau,h)\xi_k + \Gamma_r(h)u_{r,k} \tag{31}$$

with $\overline{A}_\xi(\tau,h) = A_\xi(\tau,h) + B_\xi(\tau,h)K_\xi$ and the output equation

$$z_{i,k} = C_{\Delta,i}\xi_k = [\,C_{z,i} \quad 0 \quad \ldots \quad 0\,]\,\xi_k. \tag{32}$$

We will use this model in the next section to perform a string stability analysis of the networked CACC vehicle string dynamics.

V. Model-Based String Stability Analysis

String stability of the discrete-time CACC NCS model in (31) is analyzed by using a discrete-time frequency response approach. Similar to the continuous-time frequency-domain condition given in Section II, string stability is analyzed based on the magnitude of the discrete-time string stability transfer function $(SS_{\Delta_i}(z))$, where z is the $\mathcal{Z}$-transform variable, and $\Delta_i(z) = \mathcal{Z}\{\delta_i(k)\}$. Specifically, the condition for string stability is then given as

$$|SS_{\Delta_i}(e^{j\omega})| = \left|\frac{\Delta_i(e^{j\omega})}{\Delta_{i-1}(e^{j\omega})}\right| \le 1\ \forall\omega,\ i = 1,\ldots,n \tag{33}$$

where $\delta_i \in \{q_i, v_i, a_i\}$ is the signal whose propagation along the string is of interest. To compute $SS_{\Delta_i}(z)$, we note that

$$\begin{aligned} \frac{\Delta_i(z)}{\Delta_{i-1}(z)} &= \frac{\Delta_i(z)}{u_r(z)}\left(\frac{\Delta_{i-1}(z)}{u_r(z)}\right)^{-1} \\ &= \Psi_{\Delta_{i,r}}(z)\left(\Psi_{\Delta_{i-1,r}}(z)\right)^{-1} \end{aligned} \tag{34}$$

where the discrete-time transfer functions $(\Psi_{\Delta_{i,r}}(z))$ are extracted from (31) by using

$$\Psi_{\Delta_i,r}(z) = C_{\Delta_i}\left(zI - \overline{A}_\xi(\tau,h)\right)^{-1}\Gamma_r(h), \quad i = \{1,2,\ldots,n\} \tag{35}$$

where C_{Δ_i} in (32) is such that $\delta_i = C_{\Delta_i}\xi_k$. Discrete-time transfer functions are extracted by using (35), with $\delta_i = v_i$,

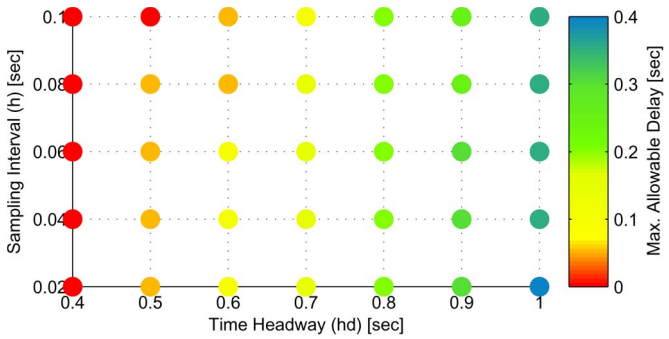

Fig. 4. Maximum allowable time delays (τ) for different sampling intervals (h) and headway time (h_d).

in order to inspect the velocity response of the vehicle string to a disturbance input u_r. Using these transfer functions and condition (33), we analyzed the string stability for a range of time headways, delays, and sampling intervals. Fig. 4 shows the results of such analysis by depicting the maximum allowable delay (τ) guaranteeing string stable operation of the CACC vehicle string for different headway-time values (h_d) and sampling intervals (h). Here, the vehicle parameters in (9) are taken as $\eta = 0.1$, with the actuator delay $\tau_{a,i} = 0.2$ s, for which a fourth-order Padé approximant was used [$\kappa = 4$ in (17)]. The bandwidth of the underlying ACC controller is taken as $\omega_{c,i} = w_{g,i}/20$, $(w_{g,i} := 1/\eta_i)$, in (11) based on speed of response and passenger comfort [11].

In Fig. 4, we conclude that, in order to achieve string stability for smaller time headways, the communication network needs to be able to guarantee smaller bounds on the delays. The analyses also show that a high sampling frequency may help to achieve string stability with relatively low intervehicle distances (h_d), while tolerating larger delays. However, from a practical point of view, increasing the sampling frequency limits the number of vehicles that can operate reliably in the same network, hence also limiting the number of vehicles in a string. Therefore, reliable operation of a CACC system involves making multidisciplinary design tradeoffs between the specification for vehicle following controller, network performance, and string stability performance criteria. The presented analyses can be used as a design tool for the designer in making these tradeoffs. In the next section, we present experimental results validating this approach toward string stability analysis.

VI. Experiments

Experimental verification of the presented NCS CACC modeling and analysis framework for string stability has been performed in a Lelystad test track with two CACC-equipped prototype vehicles of the type shown in Fig. 5, where the leader vehicle is programmed to track a predefined velocity trajectory. The main goal of these experiments is to test string stability properties for varying time headways and communication delays, in order to validate the model-based results. The choice for experiments with two CACC-equipped vehicles stems from the fact that this is the minimum number of vehicles, for which, first, string (in-)stability can be analyzed and, second, the effects of wireless communication become apparent.

Fig. 5. Prototype vehicles instrumented with CACC.

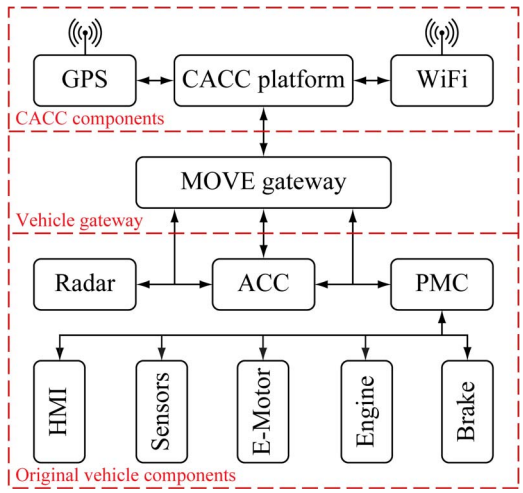

Fig. 6. Schematic representation of the test vehicle instrumentation.

A. Vehicle Instrumentation

To validate the model-based analysis results and to demonstrate the technical feasibility, the CACC control system has been implemented in two similarly adapted vehicles. The Toyota Prius III Executive was selected because of its modular setup and ex-factory ACC functionality. Fig. 6 shows a schematic representation of the components related to the experimental setup. In this figure, the CACC-related components are categorized into original vehicle components, CACC-specific components, and the vehicle gateway. These three groups of components are subsequently explained next.

By making use of original vehicle systems, only a limited number of components need to be added. The long-range radar is used to measure the relative position and speed of multiple objects, among which the preceding vehicle measurements are used for realizing the vehicle following functionality. The Power Management Control (PMC) determines the setpoints for the electric motor, the hydraulic brakes, and the engine. Finally, the Human–Machine Interface (HMI) consists of levers and a display.

Some CACC-specific components had to be implemented in the vehicle, in order to run the CACC system properly. The main component is a real-time computer platform that executes the CACC control functionality. The wireless communication

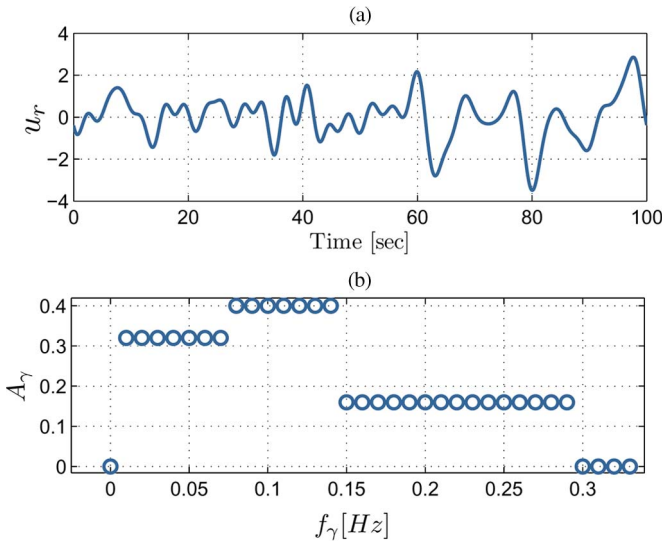

Fig. 7. Multisine velocity excitation signal for the leader vehicle. (a) Time domain. (b) Frequency domain.

device, operating according to the IEEE 802.11p standard in ad-hoc mode, allows for communication of the vehicle motion and controller information between the CACC vehicles with an update rate of 25 Hz. A GPS receiver, with an update rate of 2 Hz, has been installed to allow for synchronization of measurement data using its time stamp. Note that, however, for the particular experiments presented in this paper, a much higher clock update rate is required than that might be necessary for normal CACC operation, in order to accurately regulate the communication delays at different levels. Therefore, measurement time-stamps of test vehicles have been more accurately synchronized based on their CPU clocks with an update rate of 100 Hz.

Finally, the MOVE gateway, which has been developed by the Netherlands Organisation for Applied Scientific Research (TNO), is the interface between the original vehicle systems and the real-time CACC platform. It runs at 100 Hz, converting the acceleration setpoints u_i from the CACC platform, into vehicle actuator setpoints, such that the requested acceleration is accurately realized. The gateway also processes the vehicle sensor data and presents these to the CACC platform. Furthermore, the gateway is connected to the vehicle HMI (digital display and levers). As a result, the CACC can be operated like the ex-factory ACC system. To guarantee safe and reliable operation, the gateway also contains several safety features. The gateway employs multiple input/output for the communication with the vehicle systems; a single Controller Area Network bus is used for communication with the CACC platform. Further details on the test vehicles can be found in [11].

B. Experiment Design

The velocity trajectory for the leader vehicle has been designed as a random phase multisine excitation input [24], [25]. The time-domain velocity excitation signal depicted in Fig. 7(a) is obtained by using a multisine transformation, which allows us to synthesize test signals with predefined spectral properties, as shown in Fig. 7(b). For an accurate estimation of the string stability frequency response function (FRF) SS in (33) from

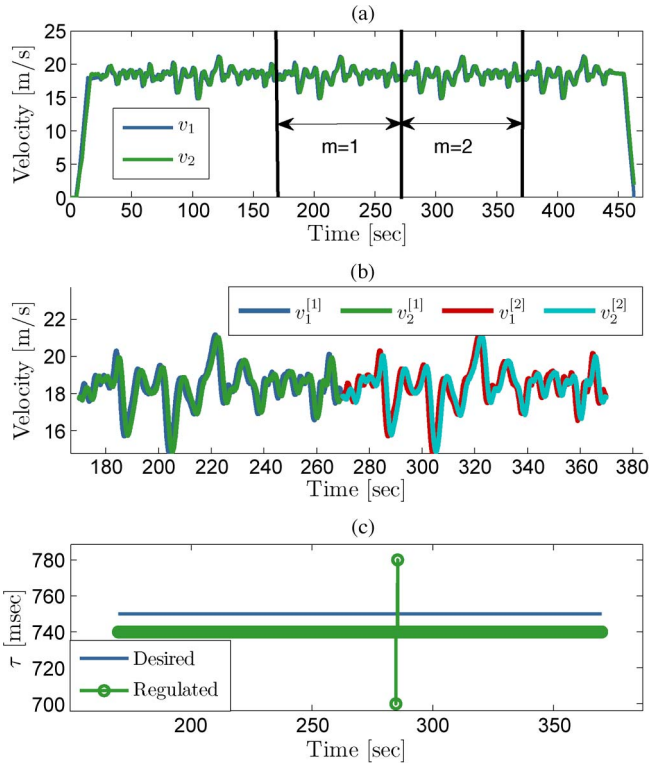

Fig. 8. Sample data set from an experiment.

the experimental data, the designed excitation signal needs to excite the frequency range of interest for the assessment of string stability. Here, the frequency bin for amplitudes A_γ is weighted at user-selected equidistant frequencies (f_γ) that are chosen on the discrete grid γf_0, such that better estimation can be achieved within a specific frequency range that is relevant for string stability (in this case, the frequency range [0, 0.3] Hz) with a sufficiently high spectral resolution (in this case, $f_0 = 0.01$). Moreover, the excitation signal is designed such that it guarantees a sufficiently high frequency-domain resolution, while vehicle-related limitations such as maximum acceleration are also respected. The corresponding N-sample multisine time-series with a period $T_0 = 1/f_0$, which is sampled at a sampling frequency $f_s = 1/T_s$, can be obtained by performing an inverse discrete fast Fourier transform of the predefined spectrum and is given by

$$u_r(nT_s) = \sum_{\gamma=1}^{F} A_\gamma \cos(2\pi f_\gamma n T_s + \phi_\gamma),\ n = [0, 1, \ldots, N-1]$$

where $N = f_s T_0$, ϕ_γ represents the random phase shifts, and $f_\gamma = \gamma f_0, \gamma \in \{1, 2, \ldots, F\}$. The ultimate velocity excitation signal used in the experiments is constructed by repeating the aforementioned excitation signal multiple times after an initial platoon formation phase, during which cars come to steady platoon operation to avoid transient behavior. The gain and phase of the estimated string stability FRF, which were obtained by averaging two periods of the multisine from the sample experimental data in Fig. 8(b), are shown in Fig. 9. In this way, the effects of road conditions and transient dynamics on the FRF estimation are reduced.

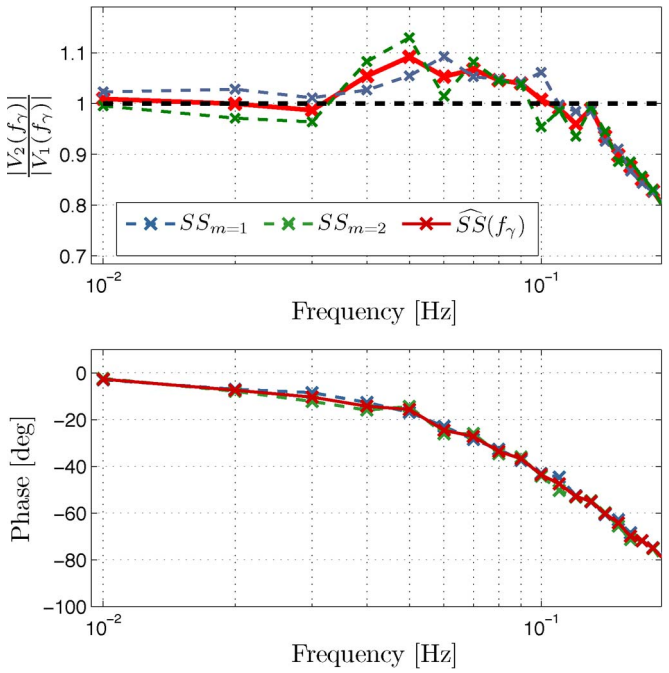

Fig. 9. Estimated frequency-response plot.

C. FRF Estimation From Experimental Data

A sample data set from the experiments is shown in Fig. 8(a). This experiment was carried out with a headway distance $h_d = 1.0$ s. The local vehicle following controller (ACC) operates at a higher frequency (100 Hz), with respect to the CACC controller, which relies on the wireless transmission frequency. CACC updates are broadcast by the leader vehicle to the follower at fixed transmission intervals ($h = 40$ ms, corresponding to a wireless communication frequency of 25 Hz). In the experiments, communication delay is artificially regulated by the receiver to certain values for assessing string stability properties experimentally for a range of constant delay levels. Fig. 8(c) shows an example of the realized communication delay over time, which is indeed approximately constant and almost equal to the "desired" $\tau = 750$ ms.

Two consecutive periods of the steady-state response [see Fig. 8(b)] are selected to compute the maximum-likelihood estimate of the string stability FRF (i.e., $\widehat{SS}_{V_i}$) in (33), as follows:

$$\widehat{SS}_{V_i}(z_\gamma) = \frac{|\hat{V}_2(z_\gamma)|}{|\hat{V}_1(z_\gamma)|} = \frac{M^{-1}\sum_{m=1}^{M}\left|V_2^{[m]}(z_\gamma)\right|}{M^{-1}\sum_{m=1}^{M}\left|V_1^{[m]}(z_\gamma)\right|} \tag{36}$$

with $z_\gamma = e^{-j2\pi f_\gamma T_s}$, where $V_i^{[m]}(z_\gamma)$ is the frequency spectrum of the time-series velocity data of the ith vehicle ($v_i^{[m]}$), and M is the number of periods of the multisine used in the estimation, as depicted in Fig. 8(b), for $M = 2$. For the validation of the CACC-model-based string stability analysis presented in Section V, experiments were carried out at representative operating points with different time headway values (h_d), where the wireless communication delay (τ) was regulated at different levels in order to support the experimental analysis of string stability for different delay magnitudes. In Figs. 10(a) and 11(a), string stability FRFs that were obtained by using the networked CACC model in (31) are compared

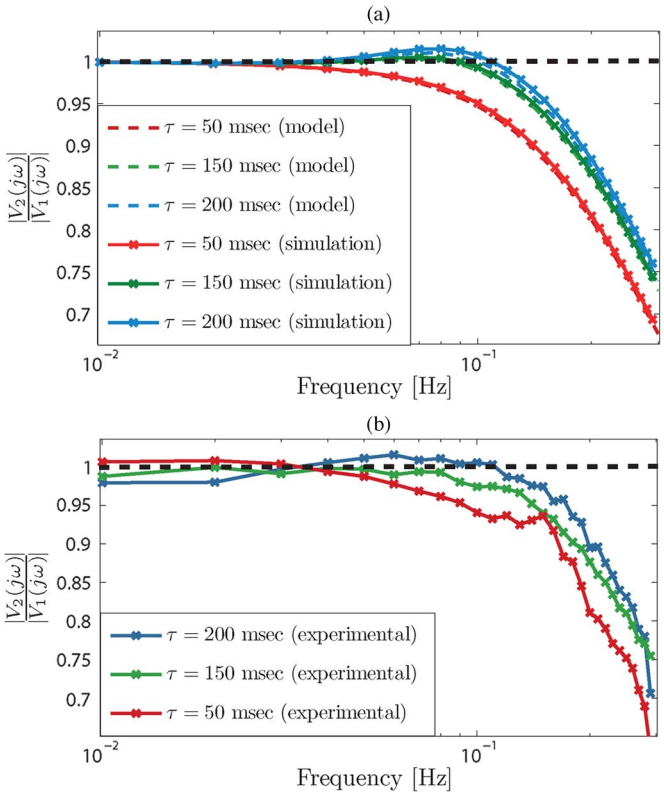

Fig. 10. Estimated FRF with $h_d = 0.6$ s.

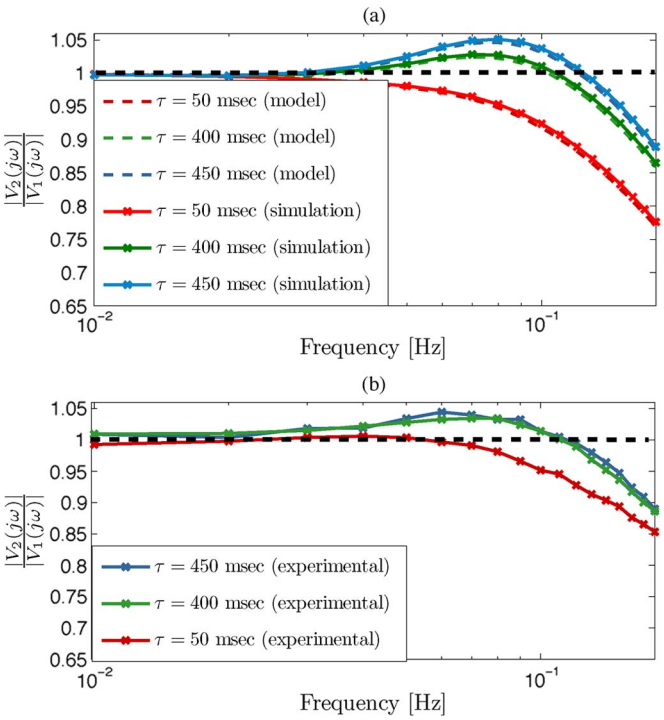

Fig. 11. Estimated FRF with $h_d = 0.8$ s.

with those obtained by FRF estimates based on simulation-based data using the CACC interconnected vehicle string model in (27). This comparison justifies the assumption made on the discretization of the input signal u_r in (28) (see also footnote[1]). These figures show that the discrete-time approach is very accurate in predicting the string stability properties of the sampled-data interconnected vehicle string model. In Figs. 10(b) and 11(b), FRF estimates based on real experiment data are presented. These experimental results show how string stability is compromised by wireless communication delays and demonstrate the reliability and practical validity of the analysis method presented in Section V.

VII. Conclusion

In this paper, we have presented an NCS framework for analyzing the effects of wireless communication between vehicles on CACC string stability performance. In particular, the effects of sampling, ZOH, and constant network delays on string stability were analyzed in detail. The results in this paper can be used as a multidisciplinary design tool to investigate tradeoffs between controller properties, wireless network specifications, and headway policies, in terms of their influence on string stability. We demonstrated the validity of the model-based analysis results by real experiments with CACC-equipped vehicles. Theoretical studies that make use of the underlying connectivity structure to derive improved scalability of the system theoretic properties for this type of platoon systems on the basis of the minimum number of vehicles are of interest for future research.

References

[1] B. van Arem, C. J. G. van Driel, and R. Visser, "The impact of cooperative adaptive cruise control on traffic-flow characteristics," *IEEE Trans. Intell. Transp. Syst.*, vol. 7, no. 4, pp. 429–436, Dec. 2006.

[2] W. Levine and M. Athans, "On the optimal error regulation of a string of moving vehicles," *IEEE Trans. Autom. Control*, vol. 11, no. 3, pp. 355–361, Jul. 1966.

[3] D. Swaroop, "String stability of interconnected systems: An application to platooning in automated highway systems," Univ. California, Berkeley, Berkeley, CA, USA, PATH Res. Rep. UCB-ITS-PRR-97-14, 1997.

[4] E. Shaw and J. Hedrick, "String stability analysis for heterogeneous vehicle strings," in *Proc. ACC*, 2007, vol. 07, pp. 3118–3125.

[5] X. Liu, A. Goldsmith, S. S. Mahal, and J. K. Hedrick, "Effects of communication delay on string stability in vehicle platoons," in *Proc. IEEE Intl. Conf. Intell. Transp. Syst.*, 2001, pp. 625–630.

[6] S. N. Huang and W. Ren, "Design of vehicle following control systems with actuator delays," *Int. J. Syst. Sci.*, vol. 28, no. 2, pp. 145–151, 1997.

[7] S. Stankovic, M. Stanojevic, and D. Siljak, "Decentralized overlapping control of a platoon of vehicles," *IEEE Trans. Control Syst. Technol.*, vol. 8, no. 5, pp. 816–832, Sep. 2000.

[8] S. Stankovic, D. Stipanovic, and D. Siljak, "Decentralized dynamic output feedback for robust stabilization of a class of nonlinear interconnected systems," *Automatica*, vol. 43, no. 5, pp. 861–867, May 2007.

[9] R. D'Andrea and G. E. Dullerud, "Distributed control design for spatially interconnected systems," *IEEE Trans. Autom. Control*, vol. 48, no. 9, pp. 1478–1495, Sep. 2003.

[10] B. Bamieh, F. Paganini, and M. Dahleh, "Distributed control of spatially invariant systems," *IEEE Trans. Autom. Control*, vol. 47, no. 7, pp. 1091–1107, Jul. 2002.

[11] J. Ploeg, B. Scheepers, E. Nunen, N. van de Wouw, and H. Nijmeijer, "Design and experimental evaluation of cooperative adaptive cruise control," in *Proc. IEEE Intell. Transp. Syst. Conf.*, Oct. 2011, pp. 260–265.

[12] J. Ploeg, S. Shladover, H. Nijmeijer, and N. van de Wouw, "Introduction to the Special Issue on the 2011 Grand Cooperative Driving Challenge," in *IEEE Trans. Intell. Transp. Syst.*, Sep. 2012, vol. 13, no. 3, pp. 989–993.

[13] M. R. I. Nieuwenhuijze, T. van Keulen, S. Öncü, B. Bonsen, and H. Nijmeijer, "Cooperative driving with a heavy-duty truck in mixed traffic: Experimental results," *IEEE Trans. Intell. Transp. Syst.*, vol. 13, no. 3, pp. 1026–1032, Sep. 2012.

[14] T. C. Yang, "Networked control system: A brief survey," in *IEE Proc. Control Theory Appl.*, Jul. 2006, vol. 153, no. 4, pp. 403–412.

[15] W. P. M. H. Heemels and N. van de Wouw, "Stability and stabilization of networked control systems," in *Networked Control Systems*, A. Bemporad, W. P. M. H. Heemels, and M. Johansson, Eds. Berlin, Germany: Springer-Verlag, 2010, pp. 203–253.

[16] P. Seiler and R. Sengupta, "Analysis of communication losses in vehicle control problems," in *Proc. Amer. Control Conf.*, 2001, vol. 2, pp. 1491–1496.

[17] D. Swaroop and J. Hedrick, "String stability of interconnected systems," *IEEE Trans. Autom. Control*, vol. 41, no. 3, pp. 349–357, Mar. 1996.

[18] G. Naus, R. Vugts, J. Ploeg, R. Molengraft, and M. Steinbuch, "String-stable CACC design and experimental validation: A frequency-domain approach," *IEEE Trans. Veh. Technol.*, vol. 59, no. 9, pp. 4268–4279, Nov. 2010.

[19] G. H. Golub and C. F. van Loan, *Matrix Computations*. Baltimore, MD, USA: The Johns Hopkins Univ. Press, 1989, pp. 557–558.

[20] M. Cloosterman, N. van de Wouw, W. Heemels, and H. Nijmeijer, "Stability of networked control systems with uncertain time-varying delays," *IEEE Trans. Autom. Control*, vol. 54, no. 7, pp. 1575–1580, Jul. 2009.

[21] N. van de Wouw, P. Naghshtabrizi, M. B. G. Cloosterman, and J. P. Hespanha, "Tracking control for sampled-data systems with uncertain sampling intervals and delays," *Int. J. Robust Nonlinear Control*, vol. 20, no. 4, pp. 387–411, Mar. 2010.

[22] S. Öncü, N. van de Wouw, and H. Nijmeijer, "Cooperative adaptive cruise control: Tradeoffs between control and network specifications," in *Proc. IEEE Intell. Transp. Syst. Conf.*, Oct. 2011, pp. 2051–2056.

[23] S. Öncü, N. van de Wouw, W. P. M. H. Heemels, and H. Nijmeijer, "String stability of interconnected vehicles under communication constraints," in *Proc. IEEE Conf. Decision Control*, Dec. 2012, pp. 2459–2464.

[24] J. Figwer, "Multisine transformation—Properties and applications," in *Nonlinear Dynamics*. Norwell, MA, USA: Kluwer, 2004.

[25] R. Pintelon and J. Schoukens, *System Identification: A Frequency Domain Approach*, 2nd ed. Hoboken, NJ, USA: Wiley, 2012.

Sinan Öncü received the B.Sc. degree in electronics and telecommunications engineering and the M.Sc. degree in mechatronics engineering from Istanbul Technical University, Istanbul, Turkey, in 2005 and 2008, respectively, and the Ph.D. degree in mechanical engineering from the Eindhoven University of Technology, Eindhoven, The Netherlands, in 2014.

He is currently with the Integrated Vehicle Safety Department, Netherlands Organization for Applied Scientific Research (TNO) Technical Sciences, Helmond, The Netherlands. His current research focuses mainly on cooperative autonomous vehicles and networked control systems.

Jeroen Ploeg received the M.Sc. degree in mechanical engineering from the Delft University of Technology, Delft, The Netherlands, in 1988. He is currently working toward the Ph.D. degree in real-time control of road vehicles for cooperative driving at the Department of Mechanical Engineering, Eindhoven University of Technology, Eindhoven, The Netherlands.

From 1989 to 1999, he was a Researcher with Koninklijke Hoogovens (currently Tata Steel), IJmuiden, The Netherlands, where his main interest was the dynamic process control of large-scale industrial plants. Since 1999, he has been a Senior Research Scientist with the Netherlands Organisation for Applied Scientific Research (TNO), Delft, The Netherlands. He is currently with the Integrated Vehicle Safety Department, TNO Technical Sciences, Helmond, The Netherlands. His current research interests include control system design for advanced driver assistance systems and path tracking of automatic guided vehicles.

Nathan van de Wouw received the M.Sc. degree (with honors) and the Ph.D. degree in mechanical engineering from the Eindhoven University of Technology, Eindhoven, The Netherlands, in 1994 and 1999, respectively.

From 1999 to 2013, he has been an Associate Professor with the Department of Mechanical Engineering, Eindhoven University of Technology. He was with Philips Applied Technologies, The Netherlands, in 2000 and the Netherlands Organisation for Applied Scientific Research, The Netherlands, in 2001. He was a Visiting Professor with the University of California, Santa Barbara, CA, USA, in 2006–2007; the University of Melbourne, Parkville, Vic., Australia, in 2009–2010; and the University of Minnesota, Minneapolis, MN, USA, in 2012 and 2013. He has published a large number of journal and conference papers and the books "Uniform Output Regulation of Nonlinear Systems: A Convergent Dynamics Approach" with Pavlov and Nijmeijer (Birkhauser, 2005) and "Stability and Convergence of Mechanical Systems with Unilateral Constraints" with Leine (Springer-Verlag, 2008).

Henk Nijmeijer (F'00) was born in 1955. He received the M.Sc. and Ph.D. degrees in mathematics from the University of Groningen, Groningen, The Netherlands, in 1979 and 1983, respectively.

From 1983 to 2000, he was with the Department of Applied Mathematics, University of Twente, Enschede, The Netherlands. Since 2000, he has been a Full Professor with the Eindhoven University of Technology, Eindhoven, The Netherlands, where he chairs the Dynamics and Control Group. He has published a large number of journal and conference papers and several books, including the "classical" Nonlinear Dynamical Control Systems (Springer, 1990), with van der Schaft; Synchronization of Mechanical Systems (World Scientific, 2003), with A.Rodriguez; Dynamics and Bifurcations of Non-Smooth Mechanical Systems (Springer-Verlag, 2004), with Leine; and Uniform Output Regulation of Nonlinear Systems (Birkhauser 2005), with Pavlov and van de Wouw.

Prof. Nijmeijer is a Board Member of the *International Journal of Control, Automatica, Journal of Dynamical Control Systems, International Journal of Bifurcation and Chaos*, *International Journal of Robust and Nonlinear Control*, *Journal of Nonlinear Dynamics*, and the *Journal of Applied Mathematics and Computer Science*. He serves as a Corresponding Editor of the *SIAM Journal on Control and Optimization*. He was a recipient of the IEE Heaviside Premium in 1990. In the 2008 research evaluation of the Dutch Mechanical Engineering Departments, the Dynamics and Control Group was evaluated as excellent regarding all aspects (quality, productivity, relevance, and viability).